



## Determination of Structure and Morphology of Gold Nanoparticle-HSA Protein Complexes

Journal:	<i>Nanoscale</i>
Manuscript ID	NR-COM-07-2015-005147.R1
Article Type:	Communication
Date Submitted by the Author:	15-Sep-2015
Complete List of Authors:	Capomaccio, Robin; JRC, European Commission, Ojea-Jimenez, Isaac; JRC, European Commission, Colpo, Pascal; European Commission Joint Research Centre, Institute for Health and Consumer Protection, Nanobiosciences Unit Gilliland, Douglas; European Commission Joint Research Centre, Institute for Health and Consumer Protection, Nanobiosciences Unit Ceccone, Giacomo; European Commission, Joint Research Centre, Institute for Health and Consumer Protection, ROSSI, Francois; European Commission, Joint Research Centre, Institute for Health and Consumer Protection, Joint Research Centre, Institute for health and consumer portection Calzolari, Luigi; JRC, European Commission,



## Determination of Structure and Morphology of Gold Nanoparticle-HSA Protein Complexes

Received 00th January 20xx,  
Accepted 00th January 20xx

Robin Capomaccio<sup>a,b</sup>, Isaac Ojea Jimenez<sup>a</sup>, Pascal Colpo<sup>a</sup>, Douglas Gilliland<sup>a</sup>, Giacomo Ceccone<sup>a</sup>, François Rossi<sup>a</sup>, and Luigi Calzolari<sup>a,†</sup>

DOI: 10.1039/x0xx00000x

www.rsc.org/

**We propose a simple method to determine the structure and morphology of nanoparticle protein complexes. By combining a separation method with online size measurements, density measurements and circular dichroism, we could identify the number of proteins bound to each nano particle and their secondary structure changes in the complex. This method provides much-needed experimental information on the interaction of proteins with nanoparticles and on the behavior of nanoparticles in biological systems.**

The structure and morphology of nanoparticle-protein complexes is important to understand the behavior of nanoparticles in biological systems and would help in the development of advanced nanomedicine<sup>1-7</sup>. Existing techniques can give information on changes in size (ultracentrifugation<sup>8</sup>, centrifugal particle sedimentation<sup>9</sup>, and light scattering-based methods<sup>10,11</sup>) or on the ligands or proteins interacting with nanoparticles (by using CD<sup>12</sup>, NMR<sup>13,14</sup> or fluorescence correlation spectroscopy<sup>15,16</sup>). But there is a lack of robust methods to determine the overall morphology and structure of NP-protein complexes. Here we show that by combining a separation technique with online size measurements, together with density measurements and circular dichroism, we could identify the number of proteins bound to each gold nanoparticle (AuNP) and their secondary structure changes in the AuNP-protein complex. This method reveals the overall morphology of the NP-protein complex directly in solution.

Citrate stabilized gold nanoparticles, were synthesized in house (see supplementary information for complete experimental details) to provide well monodispersed suspensions. The mean size and particle size distribution (PSD) were measured with electron microscopy (EM) and dynamic light scattering (DLS) (see figure S1 and S2, supplementary information) leading to respectively a diameter of 14.0 nm by EM and a hydrodynamic diameter of 17.8 nm (and a polydispersity of 0.070) by DLS. When AuNP are mixed with an excess of human serum albumin (HSA, a 66 kDa protein) there are two types of particles in solution: unbound HSA proteins and AuNP-HSA complexes. Due to their difference in size the free protein and the AuNP-HSA complex can be separated by asymmetric flow field flow fractionation (AF4)<sup>17,18</sup>, a size-separation technique able to accurately separate complex polydispersed samples<sup>19</sup>. Compared to Size Exclusion Chromatography (SEC), AF4 provides a broader dynamic range of size separation that is particularly useful for the size separation of NP-protein complexes and free proteins.

Figure 1c shows the AF4 fractogram of AuNP/HSA sample where the peaks of free HSA and AuNP-HSA complex can be readily and selectively identified using the protein autofluorescence emission at 340 nm (upon excitation at 280 nm for the protein) and the absorbance at 525 nm (specific for the localized surface resonance band of AuNP).

The second peak, belonging to the AuNP-HSA complex, has a longer exit time in the AF4 separation channel compared to the free AuNP (17 min vs. 16 min) indicating that the complex has a larger size than free AuNP. The increased size can be accurately measured by coupling the DLS online to the AF4 separation system. The data in figure 1b and 1c (blue squares) show that the hydrodynamic diameter increases from 18.5 nm (for the free AuNP) to 24.4 nm for the complex when AuNP are mixed with HSA in a 1:400 ratio.

In order to analyze the effect of the nanoparticle-protein ratio on the size and overall morphology of the AuNP-HSA complex, we have performed similar experiments at various AuNP-HSA ratios. Figure 2a shows that the retention time in the AF4 channel increases as the amount of protein per gold nanoparticle increases. The results (figure 2b) show a size of 21.4 nm for the 1:50 ratio, 22.2 nm for the 1:100 ratio, 22.7 nm for 1:200 ratio, 24.4 nm for 1:400, and 25.3 nm for the 1:1000 ratio.

<sup>a</sup> European Commission, Joint Research Centre, Institute for Health and Consumer Protection I-21027, Ispra (VA), Italy.

<sup>b</sup> Institut de Biologie et Chimie des Protéines, BMSSI-UMR 5086, Université Lyon 1, Université de Lyon, 69367 Lyon, France

†luigi.calzolari@jrc.ec.europa.eu

Footnotes relating to the title and/or authors should appear here. Electronic Supplementary Information (ESI) available: [details of any supplementary information available should be included here]. See DOI: 10.1039/x0xx00000x

These results indicate a saturation-type behaviour (figure 2b) and suggest that at saturation, human serum albumin forms a protein monolayer around gold nanoparticles to produce stable AuNP-protein complexes. It also indicates that the hydrodynamic diameter of AuNP-HSA complexes increases with the increase of protein molecules per gold nanoparticle. At saturation, HSA molecules form a monolayer of 3.4 nm in thickness around each nanoparticle. Similar values (3.5 nm) have been found in the case of HSA forming a protein corona around FePt nanoparticles as measured by fluorescence correlation spectroscopy<sup>15</sup>.

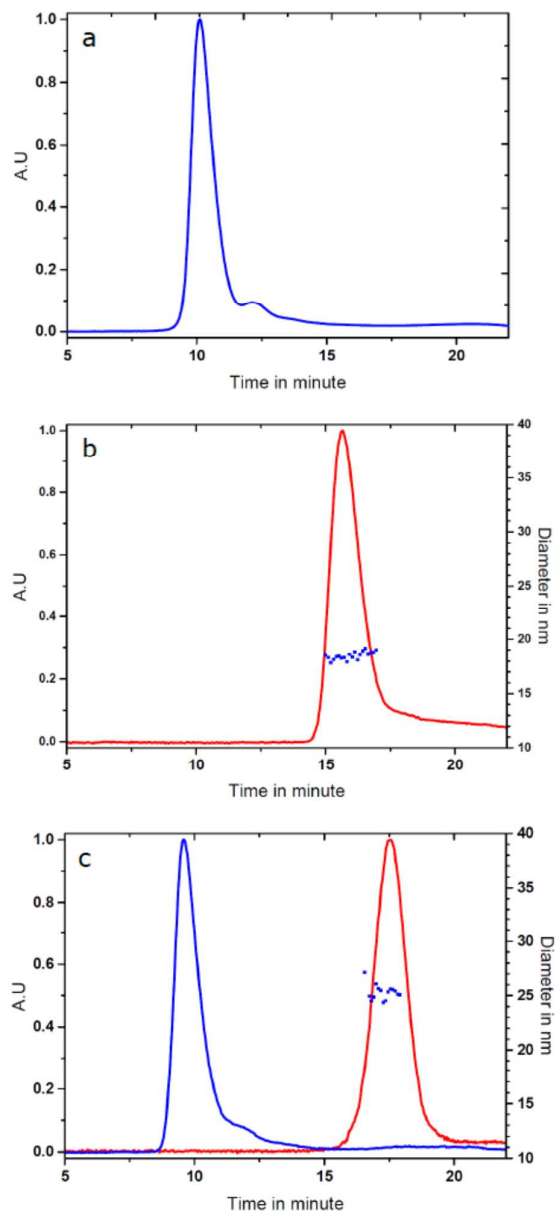


**Figure 1.** AF4-DLS measurement of AuNP-HSA samples. (a) Fluorescence detector trace (blue) of HSA alone. (b) UV-Vis detector trace at 525 nm (red, left scale), and hydrodynamic diameter (blue squares, right scale) of AuNP 15 nm alone. (c) fluorescence trace (blue, left scale), UV-Vis trace (red, left scale), and hydrodynamic diameter (blue squares, right scale) of AuNP-HSA mixture at 1:400 ratio.

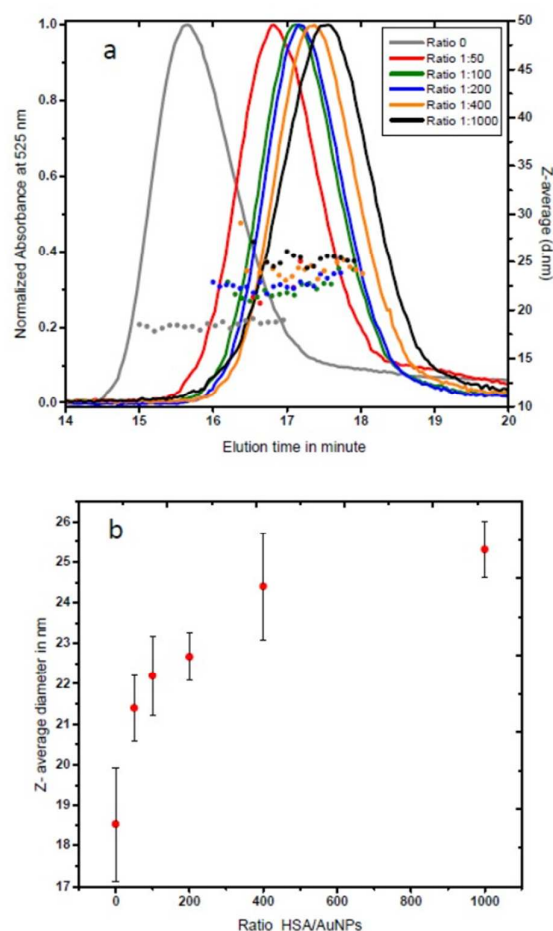


**Figure 2.** AF4-DLS measurement of AuNP-HSA complexes at various particle-protein ratios. (a) Selected part of the AF4 fractogram (UV-Vis signal at 525 nm, left scale) and corresponding diameters (Z-average, right scale) of AuNP-HSA complexes: AuNP alone (grey), 1:50 (red), 1:100 (green), 1:200 (blue), 1:400 (orange), 1:1000 (black). (b) Hydrodynamic diameter measured by AF4-DLS online for AuNP-HSA complexes at different NP-protein ratios.

The size of the complexes could allow formulating some qualitative hypothesis on the nature of the protein corona, but in order to develop a robust experimental approach we recorded differential centrifugal sedimentation (DCS) data of the various AuNP-protein samples. The time needed by each particle to reach the detector under the centrifugal field in DCS is a function of the hydrodynamic diameter and the density of the particle. Combining these measurements with the accurate size of the AuNP-HSA complexes obtained by AF4-DLS allows to determine the apparent density of the complexes at the different NP-protein ratios. Figure 3a shows that the various AuNP-HSA samples reach the detector at longer times compared to the free AuNP. By inserting the diameter measured using the AF4-DLS system (that provides accurate sizes due to the size-separation step of AF4 ensuring that monodispersed

particle populations are measured by the online DLS, see supporting information for experimental details) into equation SI-2 we could calculate the apparent densities of the complexes. The data analysis gave densities varying from 9.6 g/cm<sup>3</sup> for the free AuNP, to 6.9 g/cm<sup>3</sup>

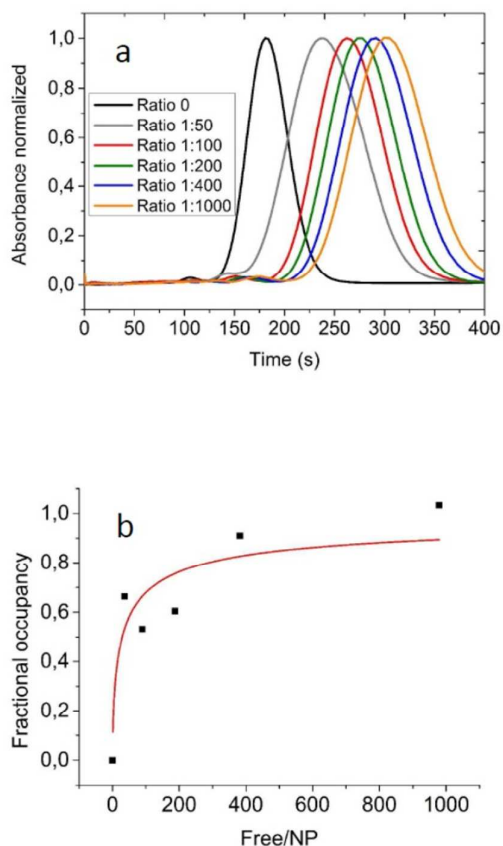


**Figure 3.** Sedimentation time and average number of HSA molecules per particle at variable AuNP-HSA ratios. (a) Centrifugal liquid sedimentation time for free AuNP (black), 1:50 ratio (grey), 1:100 ratio (red), 1:200 (green), 1:400 (blue), 1:1000 (orange). (b) Average number of HSA protein molecules per gold nanoparticles as a function of AuNP-HSA ratios (black squares) and Hill-type fitting (red curve).

for the 1:50 ratio and 4.6 g/cm<sup>3</sup> at saturation for the 1:1000 ratio (see supporting information). The somewhat surprising data for the free gold nanoparticles (compared to the 19.3 g/cm<sup>3</sup> value for the bulk gold) can be explained by the presence of citrate and water layer on AuNP surface, and the overall effect on the particle density is quite high due to the small size of the nanoparticle. Previous analysis of small AuNP with ultracentrifugation measurements has found a density of 12.5 g/cm<sup>3</sup> for AuNP of 20.3 nm<sup>20</sup>.

Combining all the experimental results (the density of the AuNP-protein complexes, together with their hydrodynamic diameter and the diameter of the core gold nanoparticle) it is possible to derive (see supporting information) the mass of the protein layer surrounding the gold core of the complex and thus to estimate the average number of proteins present in each AuNP-HSA complex. The number of HSA molecules bound to each AuNP depends on the initial NP-protein ratio (figure 3b): it starts from a minimum of 13 for the 1:50 ratio and increases up to 20 proteins for the 1:1000

ratio. Considering the surface area of one gold nanoparticle and the foot print of each HSA molecule, a single monolayer could contain a maximum of between 20 and 35 molecules based on their binding orientation on the gold nanoparticle surface<sup>21</sup>. The number of bound proteins per NP is clearly an average value, as it is safe to assume that in solution there will be a distribution in the number of bound HSA molecules to each nanoparticle for the different initial NP-protein ratios.

The experimental data can be fitted with a Hill-type equation:

$$\theta = 1/(1+(K*L)^n)$$

Where  $\theta$ : fractional occupancy of protein binding sites per NP. L: number of unbound proteins per NP. K: midpoint of the transition, number of unbound proteins per NP when 50% of the available sites are occupied. n: Hill coefficient that describe cooperative ( $n > 1$ ) or anti cooperative ( $n < 1$ ) binding behavior.

Figure 3b shows the fractional occupancy of HSA sites (at saturation, 20 bound HSA molecules per NP,) per AuNP as a function of unbound proteins in solution. The best fit of the data with the Hill equation (figure 3b, red curve) indicates that 50% of full coverage is reached when in solution there are around 35 unbound proteins per NP. The Hill coefficient of 0.6 suggests an anti-cooperative binding of HSA to gold-NP. A similar anti-cooperative behavior of HSA has been previously shown for the binding to FePt and quantum dots nanoparticles<sup>15, 16, 22</sup>.

The non-disruptive nature of the AF4-DLS technique allows recovering samples after their size separation with a simple fraction collector for further characterization. We have thus separated the AuNP-bound HSA from the unbound protein by collecting the AF4-separated peak shown in figure 1c (in red, NP-protein ratio 1:400). Using circular dichroism, we were able to acquire the CD spectra of the HSA bound protein and to monitor the changes of its secondary

structure upon binding with AuNP (figure 4).

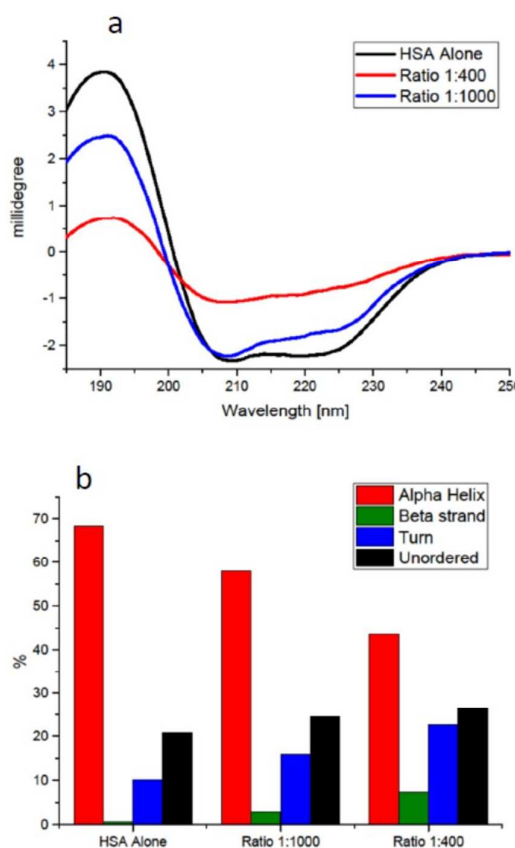


**Figure 4.** Circular dichroism spectra and secondary structure analysis of HSA for AF4-separated free HSA and AuNP-bound HSA. (a) CD spectra of free HSA (black); AuNP-HSA 1:400 (red) and 1:1000 (blue). (b) Percentage of secondary structure elements ( $\alpha$ -helix, red;  $\beta$ -strand, green; turn, blue; unordered, black) for free HSA, AuNP-HSA at 1:1000 and 1:400 ratios.

The CD spectra of HSA (figure 4a) show a clear change for the AuNP-bound protein in the far UV region between 200 and 240 nm, sensitive to the secondary structure elements present in the protein. A more detailed analysis of the two spectra using deconvolution software<sup>23</sup> allows estimating the percentage of secondary structure elements present in each CD spectrum. The data, reported in figure 4b, clearly show that there is a reduction of around 10% in the  $\alpha$ -helical content for the 1:1000 AuNP-HSA complex and of around 30% for 1:400 complex.

All these data suggest a model for the morphology of the AuNP-HSA complexes as a function of the AuNP-HSA ratio. At low ratios, the AuNP surface is not saturated by HSA molecules, 50% saturation is reached at NP-protein ratio of around 1:45, while at higher ratios HSA molecules form a single protein monolayer of 20 proteins covering the whole surface. The alpha helical content of HSA is reduced by around 30% upon binding to a gold nanoparticle, similar to the results reported in the literature<sup>24</sup> (see figure 5, blue free HSA, red bound HSA).

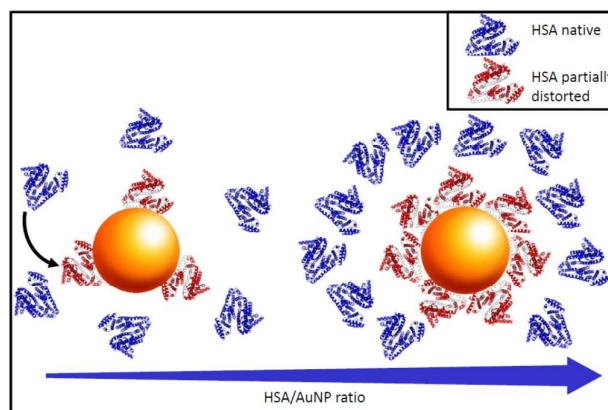


**Figure 5.** Model of the AuNP-HSA complexes. At low protein-NP ratio (left) the bound HSA occupy less than 50% of the available binding sites and their secondary structure is more distorted. At high protein-NP ratio (right) complete coverage of the nanoparticle surface is reached and the proteins are less distorted.

In addition, this methodology could also be applied to binary mixtures of proteins. By using fluorescent labelling for selective detection the amount of each protein bound to NP can be detected and information on structural changes obtained<sup>25</sup>.

A similar experimental approach can be easily extended to protein-conjugated nanoparticles, thus providing a much needed, not too complex, robust method for determining the amount and structure of bound macromolecules used to modify the properties of nanoparticles.

## Conclusions

In summary, we have demonstrated that is possible to measure the structure and morphology of nanoparticle-protein complexes. By combining a separation method with online size measurements, density measurements and circular dichroism we could identify the average number of proteins bound to each nanoparticle and the changes in the secondary structure of bound proteins. This method can be applied to any combination of NP and proteins, without the need of any fluorescence labeling. It will provide in-depth experimental information on protein-nanoparticle complexes needed for in-depth characterization of nanoparticle-protein conjugates and of the behavior of nanoparticles in biological systems.

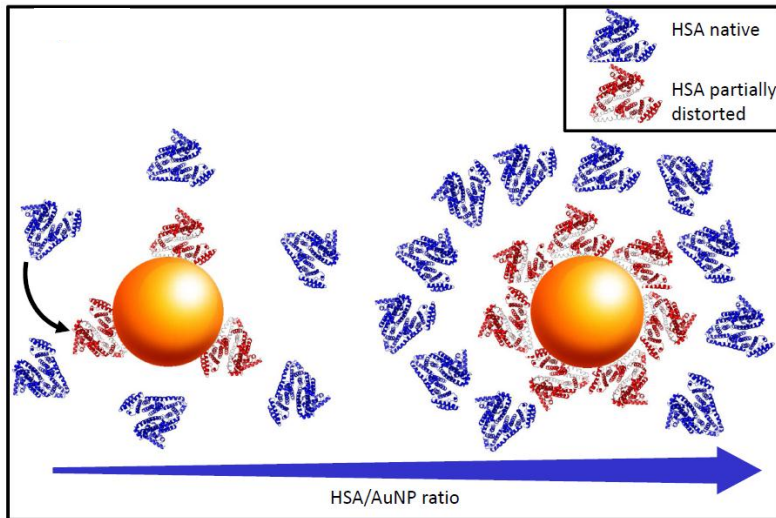
## Acknowledgements

We would like to thank Dr. Giuliano Siligardi and Dr. Rohanah Hussein of Diamond Light Source for fruitful advice and discussions related to the experimental results.

## References

1. A. E. Nel, L. Madler, D. Velegol, T. Xia, E. M. Hoek, P. Somasundaran, F. Klaessig, V. Castranova and M. Thompson, *Nat Mater*, 2009, **8**, 543-557.

2. M. Lundqvist, J. Stigler, G. Elia, I. Lynch, T. Cedervall and K. A. Dawson, *Proc Natl Acad Sci U S A*, 2008, **105**, 14265-14270.
3. Z. J. Deng, M. Liang, M. Monteiro, I. Toth and R. F. Minchin, *Nature nanotechnology*, **6**, 39-44.
4. A. Salvati, A. S. Pitek, M. P. Monopoli, K. Prapainop, F. B. Bombelli, D. R. Hristov, P. M. Kelly, C. Aberg, E. Mahon and K. A. Dawson, *Nature nanotechnology*, **8**, 137-143.
5. M. I. Setyawati, C. Y. Tay, S. L. Chia, S. L. Goh, W. Fang, M. J. Neo, H. C. Chong, S. M. Tan, S. C. J. Loo, K. W. Ng, J. P. Xie, C. N. Ong, N. S. Tan and D. T. Leong, *Nat Commun*, 2013, **4**, 1673.
6. M. I. Setyawati, C. Y. Tay, D. Docter, R. H. Stauber and D. T. Leong, *Chemical Society Reviews*, 2015.
7. C. Y. Tay, M. I. Setyawati, J. Xie, W. J. Parak and D. T. Leong, *Advanced Functional Materials*, 2014, **24**, 5936-5955.
8. R. P. Carney, J. Y. Kim, H. Qian, R. Jin, H. Mehenni, F. Stellacci and O. M. Bakr, *Nature Communications*, 2011, **2**, 335.
9. Ž. Krpetić, A. M. Davidson, M. Volk, R. Lévy, M. Brust and D. L. Cooper, *ACS Nano*, 2013, **7**, 8881-8890.
10. N. C. Bell, C. Minelli and A. G. Shard, *Analytical Methods*, 2013, **5**, 4591-4601.
11. C. Minelli, R. Garcia-Diez, A. E. Sikora, C. Gollwitzer, M. Krumrey and A. G. Shard, *Surface and Interface Analysis*, 2014, **46**, 663-667.
12. S. Laera, G. Ceccone, F. Rossi, D. Gilliland, R. Hussain, G. Siligardi and L. Calzolari, *Nano Letters*, 2011, **11**, 4480-4484.
13. L. Calzolari, F. Franchini, D. Gilliland and F. Rossi, *Nano Letters*, 2010, **10**, 3101-3105.
14. X. Liu, M. Yu, H. Kim, M. Mameli and F. Stellacci, *Nat Commun*, 2012, **3**, 1182.
15. C. Rocker, M. Potzl, F. Zhang, W. J. Parak and G. U. Nienhaus, *Nat Nano*, 2009, **4**, 577-580.
16. L. Treuel, S. Brandholt, P. Maffre, S. Wiegeler, L. Shang and G. U. Nienhaus, *ACS Nano*, **8**, 503-513.
17. J. C. Giddings, *Separation Science*, 1966, **1**, 123-125.
18. J. Giddings, *Science*, 1993, **260**, 1456-1465.
19. L. Calzolari, D. Gilliland, C. P. Garcia and F. Rossi, *Journal of chromatography*, **1218**, 4234-4239.
20. J. B. Falabella, T. J. Cho, D. C. Ripple, V. A. Hackley and M. J. Tarlov, *Langmuir*, 2010, **26**, 12740-12747.
21. L. Treuel, M. Malissek, S. Grass, J. Diendorf, D. Mahl, W. Meyer-Zaika and M. Epple, *J Nanopart Res*, 2012, **14**, 1-12.
22. P. Maffre, K. Nienhaus, F. Amin, W. J. Parak and G. U. Nienhaus, *Beilstein journal of nanotechnology*, **2**, 374-383.
23. L. Whitmore and B. A. Wallace, *Biopolymers*, 2008, **89**, 392-400.
24. S. Goy-López, J. Juárez, M. Alatorre-Meda, E. Casals, V. F. Puentes, P. Taboada and V. Mosquera, *Langmuir*, 2012, **28**, 9113-9126.
25. G. Siligardi and R. Hussain, *Enantiomer*, 1997, **3**, 77-87.



Method to measure number of proteins bound to each nanoparticle and changes in the protein structure